(51) Truscott, B.; Kane, K. M.; Idler, D. R. *Steroids* **1978**, *31*, 573–582.
(52) Schubert, K.; Schumann, G. *Endokrinologie* **1970**, *56*, 172–177.
(53) Macdonald, B. S.; Sykes, P. J.; Adhikary, P. M.; Harkness, R. A. *Steroids* **1971**, *18*, 753–766.
(54) Schubert, K.; Kaufmann, G.; Budzikiewicz, H. *Biochim. Biophys. Acta* **1969**, *176*, 170–177.
(55) We are indebted to Professor W. B. Whalley (University of London) for providing a sample of this compound. See: Emke, A.; Hands, D.; Midgley, J. M.; Whalley, W. B.; Ahmad, R. *J. Chem. Soc., Perkin Trans. 1* **1977**, 820–822.
(56) Smith, H. E.; Smith, R. G. *Org. Mass Spectrom.* **1973**, *7*, 1019–1026.
(57) Jung, G.; König, W.; Voelter, W.; Gupta, D.; Breitmaier, G.; Bierich, J. R. *Steroids* **1973**, *22*, 293–306.
(58) Heathcock, C. H.; Ellis, J. E.; McMurry, J. E.; Coppolino, A. *Tetrahedron Lett.* **1971**, 4995–4996.
(59) We thank Professor R. K. Boeckman, Jr. (Wayne State Universtiy, Detroit, Mich.) for providing a mass spectrum of this compound. See: Boeckman, Jr., R. K. *J. Am. Chem. Soc.* **1973**, *95*, 6867–6869.
(60) Audier, H. E.; Bory, S.; Fétizon, M.; Anh, N.-T. *Bull. Soc. Chim. Fr.* **1966**, *33*, 4002–4010.
(61) (a) Zürcher, R. F. *Helv. Chim. Acta* **1963**, *46*, 2054–2088. (b) Bhacca, N. S.; Williams, D. H. "Applications of NMR Spectroscopy in Organic Chemistry"; Holden-Day: San Francisco, 1964.
(62) Nussim, M.; Mazur, Y.; Sondheimer, F. *J. Org. Chem.* **1964**, *29*, 1120–1131.
(63) Physical and spectral data were in agreement with those of authentic unlabeled material.
(64) Djerassi, C.; Scholz, C. R. *J. Am. Chem. Soc.* **1948**, *70*, 417–418.
(65) The isotopic composition is given in Table II or III.
(66) Eastham, J. F.; Teranishi, R. "Organic Syntheses" Collect. Vol. IV; Wiley: New York, 1963; pp 192–195.
(67) Wilds, A. L.; Djerassi, C. *J. Am. Chem. Soc.* **1946**, *68*, 1712–1715.
(68) Lam, H.-L.; Schnoes, H. K.; DeLuca, H. F.; Reeve, L.; Stern, P. H. *Steroids* **1975**, *26*, 422–436.
(69) Barton, D. H. R.; Holness, N. J.; Klyne, W. *J. Chem. Soc.* **1949**, 2456–2459.
(70) Julian, P. L.; Meyer, E. W.; Ryden, I. *J. Am. Chem. Soc.* **1950**, *72*, 367–370.

^1H, ^2H, and ^{13}C ENDOR Studies of Labeled Bis(biphenylenyl)propenyl Type Radicals in Isotropic Solutions and in Liquid Crystals

B. Kirste, H. Kurreck,* W. Lubitz, and H. Zimmermann[1]

Contribution from the Institut für Organische Chemie der Freien Universität Berlin, Takustr. 3, 1000 Berlin 33, West Germany. *Received May 23, 1979*

Abstract: Partially deuterated and ^{13}C-labeled bis(biphenylenyl)propenyl radicals have been studied by means of ESR and ENDOR spectroscopy. Isotropic and anisotropic hyperfine contributions could be determined from measurements in isotropic solutions and in nematic and smectic phases of liquid crystals. Assignments of hyperfine coupling constants and shifts to molecular positions were achieved. Conclusions concerning molecular structure, e.g., twist angles, could be drawn by relating the experimental data to quantum mechanical calculations. These results could be confirmed by taking account of the ^{13}C hyperfine shifts determined by ESR and ^{13}C ENDOR experiments. A marked isotope effect on the β-proton hyperfine coupling could be observed when replacing ^1H by ^2H in the biphenylenyl moieties. The essential feature of the ^2H ENDOR measurements in liquid crystals is the detection of deuterium quadrupole splittings. The relaxation behavior of the different magnetic nuclei is discussed. A novel *multinuclear ENDOR standard* for checking the engineering design of a liquid-phase ENDOR spectrometer is proposed.

Introduction

Koelsch's radical (**1a**) is known to be one of the most inert, stable organic free radicals. In this respect it has attracted much attention, in view of the history of organic free radicals, for the following fact: The original publication of Koelsch was rejected in 1932 by a referee, since he did not realize that the alleged radical did not react readily with oxygen, and it took 25 years of time until the paper was accepted for publication.[2]

Koelsch's radical is unassociated even in the solid state, whereas the sterically less hindered related radical bis(biphenylenyl)propenyl (**2a**) was found to be dimeric to a high extent.[3] In the early years of ESR spectroscopy, this very radical was studied in a pioneering work of Hausser who succeeded in resolving 400 ESR lines, which is about one-third of the maximum number of lines expected from symmetry considerations.[4]

The most interesting aspect revealed by the ESR spectrum of **2a** is the exceptionally large hyperfine coupling constant of the proton at the central carbon atom, which significantly contradicts the predictions of the McConnell relation based on spin populations from HMO/McLachlan calculations.[5] The anomalously large hyperfine coupling constant could be explained by introducing a twisted allyl model and by assuming a "through-space" (hyperconjugative) interaction of the two p_z orbitals on the adjacent centers with the 1s orbital of the respective proton.[6]

In the present paper we give the results of an intense ENDOR investigation of the bis(biphenylenyl)propenyl system. In order to obtain detailed information about the isotropic and anisotropic hyperfine interactions and thus about the spin density distributions and the geometries of the radicals, we have applied elaborate techniques such as ENDOR in liquid-crystalline solvents, nonproton ENDOR, and TRIPLE resonance. For the nonproton ENDOR experiments, some deuterated and ^{13}C-labeled radicals of the bis(biphenylenyl)propenyl type had to be synthesized (see Figure 1). Our investigation consists of three parts:

(i) The isotropic ^1H, ^2H, and ^{13}C hyperfine coupling constants were measured, and the relative signs of all couplings were determined by the TRIPLE technique.[7] Moreover, the significant temperature dependence of the β-proton coupling constant of **2** was reinvestigated.

(ii) Information about the anisotropic contributions of all ^1H, ^2H, and ^{13}C hyperfine interactions was obtained by using nematic and smectic mesophases of liquid crystals as solvents. In addition, we succeeded in observing deuterium quadrupole splittings. Such splittings were recently described in three papers dealing with liquid-crystal ENDOR studies of deuterated phenalenyls[8,9] and Coppinger's radical.[10]

(iii) Recently the feasibility of nonproton ENDOR experi-

0002-7863/80/1502-0817$01.00/0

Table I. Isotropic Hyperfine Coupling Constants (in MHz)[a]

position	**1a** calcd[b]	**1a** toluene 205 K	**1a** toluene 180 K	**1a** $5CB_{iso}$[c] 309 K	**1b** $5CB_{iso}$[c] 309 K	**2a** $5CB_{iso}$[c] 309 K	**2a** $8CB_{smect}$[d] 295 K	**2c** min. oil 360 K	**2d** min. oil 360 K
α,γ-^{13}C						+38.8[e]			+40.02[i]
β-^{13}C						−33.67[f]	−33.6[g]	−34.034	
β-^{1}H						+35.544	+34.847	+36.55	+36.57
1,1′,8,8′	−5.59	−5.60	−5.85 −5.57	−5.544	−5.568	−5.648	−5.63	−0.842[h]	−0.84[h]
3,3′,6,6′	−4.77	−5.35	−5.27	−5.300	−5.288	−5.452	−5.47		
2,2′,7,7′	+0.97	+1.378	+1.376	+1.382	+1.384	+1.416	+1.411		
4,4′,5,5′	+0.16	+0.960	+1.021 +0.896	+0.964	+0.956	+1.042	+1.043	+0.188[h]	+0.19[h]
para	+0.66	+0.532	+0.55	+0.468					
ortho	+0.74	+0.324		+0.312	+0.320				
meta	−0.02	+0.10							

[a] Measured by ENDOR; accurate within +0.01 MHz, unless otherwise stated. [b] Obtained by an HMO/McLachlan calculation, using $\lambda = 1.2$, $Q_{CH}^{H} = -80$ MHz, and assuming twist angles of 30°. [c] Isotropic phase of 4-cyano-4′-pentylbiphenyl. [d] Smectic mesophase of 4-cyano-4′-octylbiphenyl. [e] Obtained from the ESR spectrum of **2d** (±0.4 MHz). [f] Obtained from the ENDOR spectrum of **2c** at (340 ± 2) K. [g] Obtained from the ESR spectrum of **2c** (±0.2 MHz). [h] Deuterium hyperfine coupling constant. [i] Measured at (395 ± 5) K in mineral oil; +39.44 MHz at (330 ± 2) K in toluene.

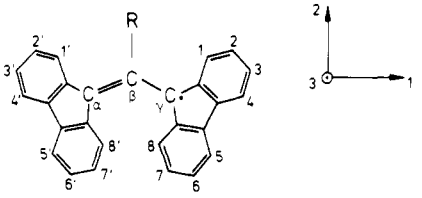

compound	R	labeled position ^{2}H	labeled position ^{13}C
1a	C_6H_5	—	—
1b	p-Cl C_6H_4	—	—
2a	H	—	—
2b	H	1-8, 1′-8′	—
2c	H	1-8, 1′-8′	β
2d	H	1-8, 1′-8′	α γ

Figure 1. Numbering scheme of compounds investigated and molecular axis system. It has to be noted that the numbering of the positions depicted in the figure will be used in all tables. The IUPAC notation is given in the Experimental Section.

ments has been demonstrated; see, e.g., ref 8, 11, and 12. The present system (**2a–2d**) appeared to be especially suitable for studying the relaxation behavior of the ^{13}C nucleus, since **2c** and **2d** contain ^{13}C nuclei in positions of intermediate or high spin density, respectively. We have investigated the dependences of the proton and nonproton ENDOR response on the different experimental parameters, e.g., temperature, microwave, and radio frequency powers.

Experimental Section

Preparation of Labeled Compounds. 1,3-Bis(biphenylenyl-d_8)-propene-*2*-^{13}C and 1,3-bis(biphenylenyl-d_8)propene-*1,3*-$^{13}C_2$ were prepared following one of the synthetic pathways for the unlabeled compound described by Kuhn et al.[13] using ethyl formate-*carbonyl*-^{13}C and perdeuteriofluorene-*9*-^{13}C, respectively, as precursors.

Fluorene-*9*-^{13}C-d_{10}. 2-Biphenylcarboxylic acid-*carboxyl*-^{13}C was prepared from 2-iodobiphenyl by Grignard reaction with $^{13}CO_2$ generated from $Ba^{13}CO_3$ (^{13}C content 90%). Subsequent reaction with sulfuric acid produced fluorenone-*9*-^{13}C and reduction with hydrazine yielded fluorene-*9*-^{13}C, which was finally exchanged twice with D_2O and prereduced PtO_2 to give fluorene-*9*-^{13}C-d_{10} (D ≈ 97–98%).[12]

Ethyl Formate-*carbonyl*-^{13}C. Sodium formate-^{13}C (1.5 g, prepared by hydrolysis of sodium cyanide-$^{13}C^{14}$) and freshly distilled triethyl phosphate (10 mL) were refluxed for 30 min. Ethyl formate-*carbonyl*-^{13}C was distilled from the reaction mixture at room temperature using a high vacuum line and liquid nitrogen cooled traps. Subsequent fractionation under high vacuum at room temperature yielded 1.2 g (70%) of ethyl formate-*carbonyl*-^{13}C.

1,3-Bis(biphenylenyl-d_8)propene-*2*-^{13}C and 1,3-Bis(biphenylenyl-d_8)propene-*1,3*-$^{13}C_2$. Fluorene-*9*-^{13}C-d_{10} was converted to the lithium salt, which was allowed to react with ethyl formate using a molar ratio of 4:1 (or fluorene-d_9–Li and ethyl formate-*carbonyl*-^{13}C, respectively) to yield the corresponding bis(biphenylenyl)propene. After recrystallization from benzene/hexane, the melting points were 201–202 °C. The mass spectra of the labeled propenes showed the expected M^+ peaks. The degree of incorporation was 97–98% D; ≈90% ^{13}C; ≈80% $^{13}C_2$.

Preparation of Samples. 1,3-Bis(biphenylenyl)-2-(4-chlorophenyl)propenyl has been synthesized according to Kuhn and Neugebauer.[15] The free propenyl radical **2** and the dimers of radicals **1** were prepared from the propenes following the procedure given in ref 13. Radical solutions were obtained by dissolving the respective monomeric or dimeric solids in toluene, or mineral oil (Shell Ondina G17), or in liquid crystals. Subsequently, the solutions of the radicals were carefully degassed on a high vacuum line. The liquid crystals 4-cyano-4′-pentylbiphenyl (nematic phase 295–308 K) and 4-cyano-4′-octylbiphenyl (smectic A phase 294–307 K, nematic phase 307–314 K) were synthesized according to ref 16.

Instrumentation. ESR spectra were recorded on a Bruker ER 220 D. ENDOR and TRIPLE spectra were recorded on a broad-band spectrometer that consists basically of an AEG-20XT spectrometer and of a continuous wave ENDOR accessory built up in this laboratory. Our ENDOR/TRIPLE arrangement was recently described in some detail.[17] The temperature was varied with an AEG temperature control unit (accuracy ±1 K).

Results and Discussion

Isotropic Solution Measurements. Koelsch's Radical. ENDOR spectra of **1a** and **1b** have been taken in the isotropic phase of 4-cyano-4′-pentylbiphenyl (5CB) and also in toluene (**1a** only). The relative signs of all hyperfine couplings could be determined by means of the TRIPLE resonance technique; the largest coupling was assumed to be negative. The experimental hyperfine couplings are collected in Table I, together with the results obtained from an HMO/McLachlan calculation and McConnell's relation (using $Q_{CH}^{H} = -80$ MHz). It has to be noted that the calculated hyperfine couplings for the protons in the biphenylenyl moieties are essentially inde-

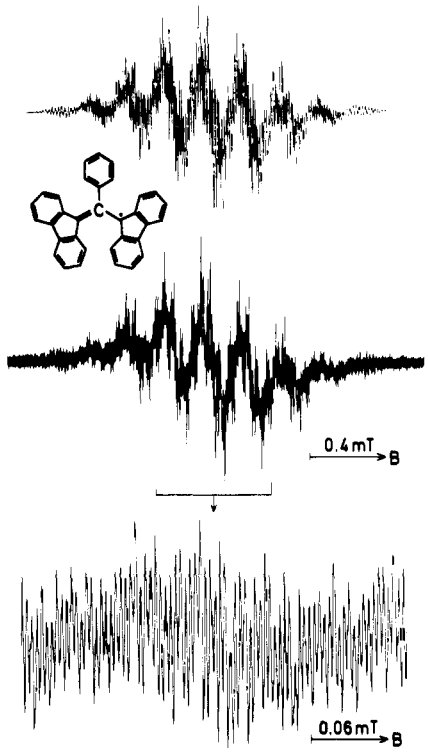

Figure 2. Experimental (center; toluene, 250 K) and simulated ESR spectrum (top) of Koelsch's radical **1a.** Bottom: central part of the high-resolution ESR spectrum, line width 2.0 μT ($c \simeq 10^{-5}$ mol/L, microwave power 0.02 mW, 0.6 μT amplitude of the 12.5-kHz field modulation). Note that the simulation which is based on the ENDOR data (obtained at 205 K; see Table I) depends critically upon the number of protons assigned to the coupling constants.

pendent of the twist angles (twist angles of 30° were assumed for the phenyl and the biphenylenyl groups). Thus, the isotropic couplings provide no information concerning deviations from planarity; however, some conclusions may be drawn from the shifts measured in nematic mesophases (vide infra).

The assignment of the hyperfine couplings to the phenyl or biphenylenyl moieties is based on a comparison with the corresponding radical without a phenyl substituent at the central carbon atom (**2a**). For the assignment to specific positions within the biphenylenyl groups, the ordering suggested by the MO calculation has been taken as a basis. This is supported in part by the TRIPLE results; however, the assignment to positions 1 and 3 or 2 and 4 might be interchanged.

A tentative assignment of the proton couplings to specific positions in the phenyl group is given in ref 18, but is not in agreement with our results. The couplings of about 0.5 and 0.3 MHz both have positive signs. This is to be expected for the ortho and para protons of a phenyl ring attached to a carbon atom bearing *negative* spin population; compare the calculated values (Table I). Moreover, in the para-chloro substituted compound only the ENDOR lines belonging to the smaller of these two couplings show up. For an unambiguous assignment, deuteration would strictly be required, but our recent study of 2-chlorophenalenyl has revealed that chloro substitution in odd alternant neutral radicals does not noticeably affect the spin density distribution.[19] The ENDOR lines belonging to the meta protons are not easily found, but in the ENDOR and TRIPLE spectra taken in dilute toluene solutions two lines of low intensity close to the free proton frequency show up, corresponding to a coupling of +0.10 MHz. This finding is somewhat surprising, since a small *negative* coupling is expected on the basis of the calculation. It should be noted that the experimental ESR spectrum is well reproduced by a simulation using the coupling constants obtained from ENDOR (see Figure 2), thus supporting the above assignment.

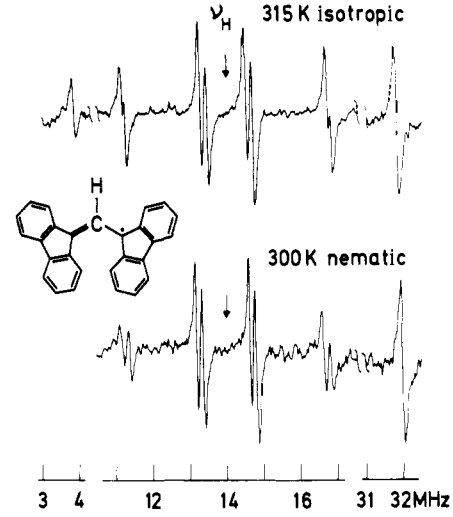

Figure 3. ENDOR spectra of **2a** in the isotropic (top) and in the nematic phase (bottom) of 4-cyano-4′-pentylbiphenyl ($B_N' = 0.5$ mT in the rotating frame).

The line-shape effects displayed by the ENDOR line at about 16.7 MHz described by Watanabe[6] have been confirmed by our measurements. Additionally, we found a splitting of the ENDOR line at about 14.5 MHz on lowering the temperature (see Table I). These effects are characteristic of an intramolecular dynamic process caused by hindered rotation of the biphenylenyl groups.[6] In ref 6, the inequivalence of the protons observed at low temperatures is ascribed to different twist angles for the two biphenylenyl groups (assuming, e.g., $a_1 = a_8 \neq a_{1'} = a_{8'}$). Another possibility, the inequivalence of "interior" and "exterior" protons (i.e., $a_1 = a_{1'} \neq a_8 = a_{8'}$), seems more reasonable; we have observed similar phenomena in the investigation of dynamic processes in galvinoxyls.[10,11,20,21]

Bis(biphenylenyl)propenyl Radicals. Spectra of **2a** to **2d** could not be obtained far below room temperature because of the substantial extent of dimerization. According to the ENDOR resonance condition $\nu_{ENDOR} = |\nu_H \pm a_i/2|$, the lines of the protons of the biphenylenyl moieties of **2a** are equally spaced around ν_H separated by a_i because $|a_i/2| < \nu_H$ is valid; see Figure 3 (top). However, the most striking feature in the ENDOR spectrum of this radical is provided by the large allyl β-proton hyperfine coupling of about 35 MHz. In fact, this is presumably the first example for a liquid-phase ^{1}H ENDOR spectrum with $|a_i/2| > \nu_H$; hence these ENDOR lines are centered around $a_i/2$ separated by $2\nu_H$. Moreover, the experimental value of ν_H shows a marked second-order shift of (+30 ± 5) kHz which can be interpreted using $\delta\nu = \langle a^2 \rangle / (4\nu_e)$.[22]

The β-proton hyperfine coupling in radicals **2** exhibits a significant temperature dependence. An ESR study of this effect has been described in ref 6, but no quantitative interpretation is given. We have accurately measured the temperature coefficient of the β-proton coupling in the isotropic phase of 4-cyano-4′-octylbiphenyl (8CB) by means of ENDOR, $da/dT = (+10.4 \pm 0.2)$ kHz/K in the temperature range of 315–345 K; no deviation from linearity was found within experimental error.

Regarding the labeled compounds with perdeuterated biphenylenyl groups (**2b–2d**), two pairs of ^{2}H ENDOR lines could be detected in mineral oil or in the isotropic phase of 5CB. Small splittings of these lines that were expected on the basis of the respective ^{1}H ENDOR spectrum could not be resolved in the isotropic phase, thus preventing the determination of the

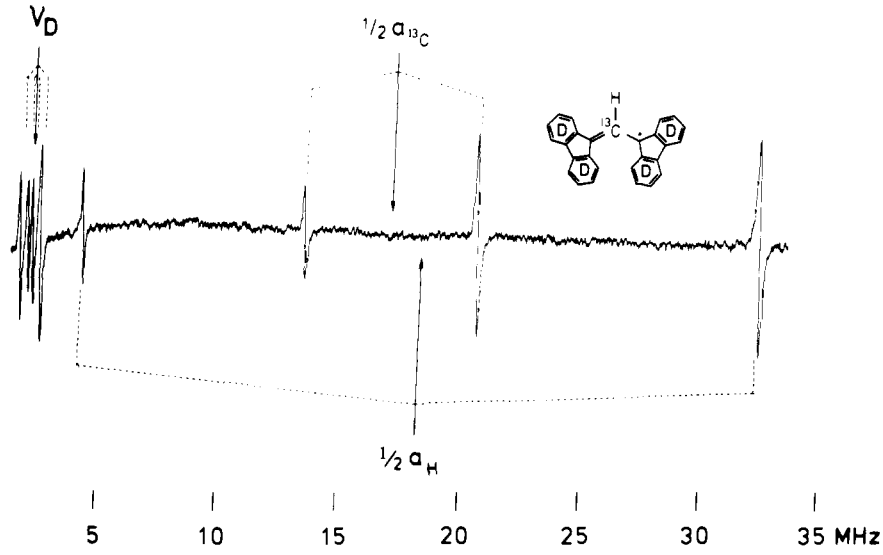

Figure 4. Multinuclear ENDOR spectrum of **2c** in mineral oil at 360 K; microwave power 22 mW. Owing to the experimental arrangement of the rf channel,[7,17] the NMR power is frequency dependent; it is 0.75 mT (rotating frame) at 14 MHz. Base-line drifts at lower frequencies are due to the lack of ESR field modulation; radio frequency modulation (10 kHz), amplitude 50 kHz.

a_H/a_D ratios. Furthermore, the β-proton hyperfine coupling constant of **2** shows an interesting isotope effect: The coupling constant is decreased by (120 ± 15) kHz in the labeled form with perdeuterated biphenylenyl groups. In order to eliminate experimental errors that might be caused by small differences of the sample temperatures, a mixture of **2c** and the unlabeled compound **2a** was investigated, allowing a selective setting of the ESR during the ENDOR measurements. In the temperature range of 315–345 K (solvent: isotropic phase of 8CB), no temperature dependence of the isotope effect was found within experimental error.

In radical **2c** all three kinds of nuclei present (^{1}H, ^{2}H, ^{13}C) could be detected with an almost equal intensity of the high-frequency lines by adjusting the experimental parameters (microwave and radio frequency powers, especially temperature). This multinuclear ENDOR spectrum ranging from 1 to 34 MHz is reproduced in Figure 4. Two ^{2}H ENDOR line pairs show up equally spaced around the free deuterium frequency at ν_D = 2.15 MHz; the β-proton and ^{13}C ENDOR lines are centered about one-half the respective hyperfine coupling constant $a_i/2$ spaced by $2\nu_N$. The smaller amplitudes of the low-frequency lines are due to lower effective radio frequency (rf) fields at the nuclei caused by the hyperfine enhancement factor.[23] The hyperfine splitting constants of **2c** are collected in Table I; the signs were determined by TRIPLE resonance.

It is a common property of the type of radicals described so far that the ESR transitions can be saturated with small microwave fields.[4] However, a quite different behavior was found for radical **2d.** Thus, only at enhanced microwave power could ^{1}H and ^{2}H ENDOR lines of **2d** be registered (mineral oil, 360 K). Moreover, the ^{13}C ENDOR lines (α, γ positions) are only detectable at considerably higher temperatures, rf fields, and rf modulation amplitudes. In **2d** the ^{13}C ENDOR line width is considerably larger than that in **2c.** At an external field of about 1 mT (rotating frame), line widths are 450 kHz (**2d**) and 200 kHz (**2c**), respectively. The protons and deuterons in both radicals exhibit comparable line widths within experimental error. The hyperfine couplings of **2d** are also given in Table I; the sign of the ^{13}C coupling was inferred from liquid crystal measurements (vide infra). In contrast to the anisotropic contributions, the isotropic ^{13}C hyperfine coupling constant for the α,γ positions proved to be larger by only about 20% than that for the β position. Actually, a calculation using the Karplus–Fraenkel relation[24] yielded $a_{calcd}(\alpha,\gamma\text{-}^{13}C)$ = +26.9 MHz and $a_{calcd}(\beta\text{-}^{13}C)$ = −27.9 MHz. The deviation from the experimental data is probably due to the neglect of the angular dependence of the Q parameters in the Karplus–Fraenkel treatment; for a similar observation, see ref 11.

β-Proton Hyperfine Coupling Constant. As was pointed out in the foregoing section, the β-proton hyperfine coupling of the radicals **2** is anomalously large and, in fact, contradicts the predictions of the simple McConnell relation on the basis of a McLachlan calculation (a_{calcd} = +6.2 MHz). However, for steric reasons the radical cannot be planar, thus causing direct overlap of the p orbitals on the α and γ carbon atoms of the allyl system with the hydrogen 1s orbital. Similar explanations have been given for the β proton coupling in the cyclohexadienyl radical,[25] and for galvinoxyl (Coppinger's radical),[26] the appropriate equation for the hyperfine coupling is:

$$a_\beta^H = Q_{CH}{}^H\rho_\beta + 4B_2{}^H\rho_\alpha \cos^2(90° - \theta) \qquad (1)$$

where θ is the twist angle of the biphenylenyl groups. Assuming $Q_{CH}{}^H$ = −80 MHz, $B_2{}^H$ = 138 MHz,[27] and the respective McLachlan spin populations ($\rho_\alpha = \rho_\gamma$ = 0.258, ρ_β = −0.079), one obtains a twist angle of θ = 27°. In ref 6, θ is claimed to be 37°, but in our opinion this value was obtained from an inappropriate equation. Moreover, such a large twist angle would not be in accordance with our studies in the nematic phase, vide infra.

The temperature dependence of β-proton coupling constants due to torsional oscillations is conventionally interpreted on the basis of the Stone–Maki model,[28] for applications see, e.g., ref 21 and 29. Since the molecule is no static species but rather undergoes torsional oscillations about equilibrium twist angles θ_0, the $\cos^2$ term in eq 1 should strictly be replaced by a temperature-dependent average. In the classical limit one obtains:

$$\overline{a_\beta^H} = \frac{\int_{-\pi}^{\pi} a_\beta^H(\theta) \exp[-V(\theta)/kT]\, d\theta}{\int_{-\pi}^{\pi} \exp[-V(\theta)/kT]\, d\theta} \qquad (2)$$

where $a_\beta^H(\theta)$ is given by eq 1 and $V(\theta)$ is the potential function for a rotating group with C_2 symmetry:[29]

$$V(\theta) = \frac{V_0}{2}[1 - \cos 2(\theta - \theta_0)] \qquad (3)$$

Table II. Experimental and Calculated Coupling Constant Shifts (in MHz) [a]

position	1a 5CB$_{nem}$	1b 5CB$_{nem}$	2a 8CB$_{smect}$	2a 5CB$_{nem}$	2a calcd[b]
α,γ-^{13}C				−11.6[c]	−11.17
β-^{13}C			+5.2[c]	+5.0[c]	+5.17
β-^{1}H			+1.20	+1.06[d]	+1.09
1,1′,8,8′	−0.07	−0.05	−0.04	−0.01	+0.25
3,3′,6,6′	+0.20	+0.18	+0.29	+0.24	+0.16
2,2′,7,7′	+0.13	+0.12	+0.24	+0.22	+0.20
4,4′,5,5′	+0.16	+0.14	+0.28	+0.24	+0.30
para	(+0.06)				
ortho	(+0.22)	+0.30			

[a] The experimental data were obtained from ENDOR measurements; solvent; nematic phase of 4-cyano-4′-pentylbiphenyl (5CB) or smectic phase of 4-cyano-4′-octylbiphenyl (8CB), 295 K. [b] Calculated with $O_{33} = -0.33$ and the tensor components from Table III. [c] Obtained from the ESR spectra of **2c** or **2d**, respectively. [d] Shift relative to the isotropic coupling measured in 8CB; see text.

Table III. Diagonal Components of the Anisotropic Hyperfine Tensors of **2a** (in MHz)[a]

position	A'_{11}	A'_{22}	A'_{33}
α,γ-^{13}C	−19.7615	−14.0981	33.8596
β-^{13}C	9.4722	6.1969	−15.6691
β-^{1}H	3.5714	−0.2778	−3.2937
1,1′	−0.3239	1.4548	−1.1310
2,2′	0.4225	0.2173	−0.6398
3,3′	2.6136	−2.1399	−0.4736
4,4′	0.9664	−0.0743	−0.8921
5,5′	0.7507	0.1739	−0.9246
6,6′	−1.8133	2.3235	−0.5102
7,7′	−0.0595	0.6278	−0.5684
8,8′	1.6581	−1.2974	−0.3607

[a] Calculated with McLachlan spin populations (using $\lambda = 1.2$), assuming twist angles of 25°, standard bond lengths ($R_{C-C} = 139.7$ pm, $R_{C-H} = 108.5$ pm), and $Z_{eff}(C) = 3.18$; see text. For the axis system, see Figure 1.

A fit to the experimental data yielded $V_0 = (39 \pm 2)$ kJ/mol for the potential barrier and $\theta_0 = (25.4 \pm 0.1)°$. (The errors have been estimated from the fit procedure; contributions due to possibly incorrect parameters used in eq 1 are not included.)

To conclude the discussion of the β-proton hyperfine coupling constant, some comment will be given concerning the significant isotope effect described above. In principle, deuteration might affect the π-spin density distribution. In the present case, however, this possibility need not be considered, because **2** is an odd alternant hydrocarbon radical.[30] Looking for another explanation, the effects of deuteration on the torsional oscillations will be considered. Perdeuteration increases the moment of inertia of a biphenylenyl group by about 10%. According to the model of Das,[31] this would reduce the frequency of the torsional vibration in the classical approximation $\nu_{osc} = (V_0/2I_{eff})^{1/2}/2\pi$ by about 5% and might affect the amplitude or, more specifically $\langle\cos^2\theta\rangle$. The latter effect, although of importance for the zero-point vibration, is negligible at room temperature since $h\nu_{osc} \ll kT$. The frequency of the torsional vibration cannot directly affect the β-proton hyperfine coupling, but might influence the equilibrium geometry, i.e., θ_0. In fact, a small reduction of the equilibrium twist angle by 0.07° would completely account for the observed isotope effect.

Liquid-Crystal Measurements. On passing to the nematic mesophase, radicals dissolved in a liquid crystal are partially aligned, causing a shift in the observed hyperfine splittings due to contributions from the anisotropic hyperfine interaction:[32]

$$\Delta a = O_{33}A'_{33} + \tfrac{1}{3}(O_{11} - O_{22})(A'_{11} - A'_{22}) \qquad (4)$$

where O_{ii} and A'_{ii} are the elements of the traceless ordering and anisotropic hyperfine tensors, respectively, and the principal axis system of the ordering matrix is chosen as the molecular axis system. While nematic phases are macroscopically aligned by a magnetic field of about 0.3 T, this is not the case for smectic phases owing to the high macroscopic viscosity.[33] However, a monodomain sample of a smectogen like 4-cyano-4′-octylbiphenyl, which also produces a nematic phase, is easily obtained by employing a magnetic field to align the nematic phase and slowly lowering the temperature until the smectic phase is formed.[10,34] Smectic A phases offer the advantage of arbitrary control of the direction of orientation; the observed hyperfine splitting depends upon the angle γ between the director and the magnetic field:[35]

$$|\bar{a}(\gamma)| = [\tilde{A}_\perp{}^2 + (\tilde{A}_\parallel{}^2 - \tilde{A}_\perp{}^2)\cos^2\gamma]^{1/2} \qquad (5)$$

where $\tilde{A}_\parallel = a + \Delta a$, $\tilde{A}_\perp = a - (1/2)\Delta a$, and Δa is given by eq 4. Thus, two measurements at $\gamma = 0°$ and $\gamma = 90°$ yield the shift Δa and the actual isotropic hyperfine coupling constant, which is of special value in the case of strongly temperature-dependent couplings.[10]

^{1}H and ^{13}C Hyperfine Splitting Shifts. Figure 3 (bottom) shows the ENDOR spectrum of **2a** in the nematic phase of the liquid crystal 4-cyano-4′-pentylbiphenyl (5CB); the observed coupling constant shifts are collected in Table II. **2a** has also been studied in the smectic A phase of 4-cyano-4′-octylbiphenyl (8CB). In fact, the β-proton hyperfine coupling of **2a** provides an excellent example of the advantages offered by the smectic mesophase. As was mentioned above, this coupling shows a significant temperature dependence. In a nematic phase experiment, the shift can only be evaluated by reference to a measurement at a higher temperature or in another solvent. In the nematic phase of 5CB, $a_\beta = 35.91$ MHz (295 K) was measured, corresponding to a shift of +0.37 MHz if no correction is made. This value is increased by about 0.17 MHz if the temperature dependence of the isotropic hyperfine coupling observed in the isotropic phase is extrapolated to the nematic phase. However, the investigation in the smectic phase of 8CB shows that this way of correction does not give reliable results. At the same temperature, $\Delta a = +1.20$ MHz and $a = 34.85$ MHz were obtained, to be compared with an extrapolated value of $a = 35.40$ MHz. The decrease of the isotropic coupling constant by 0.55 MHz might be explained by a decrease of the torsional angle of the biphenylenyl groups by about 0.3°, suggesting that a more planar conformation of the radical is preferred in the smectic phase of the liquid crystal.

The components of the anisotropic hyperfine tensors (see Table III) were calculated according to the theory of McConnell and Strathdee,[35] using the modified equations for twisted radicals given in ref 32. For carbon-13, 181.6 MHz was assumed for the component in the z direction for unit spin population in the $2p_z$ orbital.[36] Assuming $O_{11} = O_{22}$ ($\Delta a = O_{33}A'_{33}$), the best fit to the experimental data of **2a** in 5CB was obtained for $O_{33} = -0.33 \pm 0.02$ (see Table II), taking the averages of the hyperfine components for positions 1 and 8, 2 and 7, etc. No improvement was achieved when allowing different values for O_{11} and O_{22}. The agreement between experimental and calculated values appears to be satisfying, except for position 1. This discrepancy might be due to inaccuracies of the applied spin populations or to inherent difficulties of the McConnell-Strathdee treatment;[32,37] moreover, the respective ENDOR lines show a broadening that is probably caused by hindered internal rotation of the biphenylenyl groups. It is noteworthy that the ^{13}C hyperfine splitting shifts

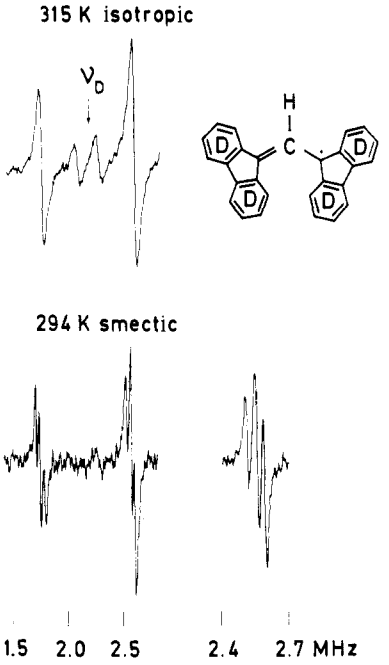

Figure 5. ^{2}H ENDOR spectra of **2b** in the isotropic (top) and in the smectic phase (bottom; γ = 0°) of 4-cyano-4′-octylbiphenyl. Bottom right: high-frequency ^{2}H ENDOR lines recorded under high-resolution conditions on an expanded frequency scale (B_N' = 0.5 mT in the rotating frame, 5-kHz amplitude of the 5-kHz frequency modulation).

confirm the results concerning the twist angles derived from the magnitude of the isotropic β-proton coupling, because larger twist angles would require smaller shifts for the α carbon (e.g., $\Delta a(\alpha\text{-}^{13}C) = -6$ MHz for θ = 37°) and vice versa.

The shifts observed for **1a** and **1b** are smaller by about 30% than those of **2a** under identical experimental conditions (Table II). This observation is readily accounted for by assuming larger twist angles caused by the phenyl substituent and a correspondingly lower degree of alignment (e.g., θ = 30° and $O_{33} = -0.20$), although a reliable quantitative interpretation is not possible. All of the shifts are rather small, except for the phenyl ortho protons, which might be ascribed to an interaction with the π system of the biphenylenyl moieties. The ENDOR lines assigned to the ortho and para phenyl protons of **1a** could not be resolved in the nematic phase.

Deuterium Quadrupole Splittings. Quadrupole coupling of a deuterium nucleus (I = 1) may give rise to a splitting $\delta_Q = 2|\Delta\nu_Q|$ of the ^{2}H ENDOR lines:[8]

$$\nu_{ENDOR} = |(\nu_D \pm \bar{a}/2) \pm \Delta\nu_Q| \quad (6)$$

$$\Delta\nu_Q = Q'\left[O_{xx} + \frac{1}{3}\eta(O_{yy} - O_{zz})\right] \quad (7)$$

where $Q' = (3/4)e^2q_{xx}Q/h$ and $\eta = (q_{yy} - q_{zz})/q_{xx}$, referring to the principal axis system of the C–D fragment with the x axis along the bond direction.

Experimentally, such a splitting was observed for the ^{2}H ENDOR lines belonging to the larger two couplings of **2b** in the nematic phase of 5CB and in the smectic phase of 8CB (see Figure 5). (The ^{2}H ENDOR lines belonging to the smaller couplings were hardly observable due to signal-to-noise problems.)

Considering the results of the ^{1}H ENDOR spectra (Figure 3), one expects two high-frequency ^{2}H ENDOR lines. This splitting is not resolved in the isotropic, but in the nematic phase due to different shifts and smaller line widths. Additionally, each line is split by the ^{2}H quadrupole interaction. It is obvious from Figure 5 that the ^{2}H ENDOR line shows only a splitting into *three* lines (splittings: 43 and 33 kHz for 8CB, smectic, γ = 0°, 295 K; 35 and 31 kHz for 5CB, nematic, 295 K; ±2 kHz), since accidentally the quadrupole splittings are approximately equal to half the difference of the two deuterium hyperfine splittings (38 or 34 kHz, respectively, calculated from the proton data). Although the degree of ordering of the radicals is about the same or even higher, the observed quadrupole splittings are somewhat smaller than those reported for the phenalenyl system (42.2 kHz for $O_{33} = -0.30$).[8] In contrast to phenalenyl, **2b** is not a planar system, and the deviation can be accounted for if the torsional angle of the biphenylenyl groups is taken into consideration. A quantitative treatment, however, is not possible without specific deuterium labeling and a precise knowledge of the ordering parameters.

ENDOR Study of Spin Relaxation. As is well known from theoretical work, successful ENDOR experiments call for saturation of the electron and nuclear spin transitions and optimization of the experimental conditions, i.e., concentration, viscosity of the solvent, and temperature, in such a way that "relaxation resistances" become as small as possible in the energy level system of the radical.[22] ENDOR amplitudes and line widths are strongly dependent on electron and nuclear relaxation arising from the modulation of the different magnetic interactions by Brownian rotational diffusion.[12,36] Neglecting cross-relaxation effects, the maximum ENDOR enhancement is obtained at equal electron and nuclear spin-lattice relaxation rates $W_e = W_N$. Since $W_N/W_e \propto \tau_c^2 \propto (\eta/T)^2$, i.e., the ENDOR response depends markedly on the correlation time τ_c and thereby on the viscosity η and the temperature T of the solution.[38]

Electron spin relaxation (W_e) is caused by g-factor anisotropy, spin-rotational interaction, and also by electron–nuclear dipolar interactions. The main source of the nuclear relaxation rate W_N is the modulation of the electron–nuclear dipolar interaction; the effect of quadrupolar interactions can be neglected in the case of deuterium nuclei.[8] Nuclear relaxation is therefore determined by τ_c and the sum of the squared elements of the anisotropic hyperfine coupling tensor, $W_N \propto \mathrm{Tr}(A'^2)\tau_c$, because $\omega_N^2\tau_c^2 \ll 1$. Since deuterons, protons, and ^{13}C nuclei in the bis(biphenylenyl)propenyl radicals exhibit different anisotropies, their relaxation behavior is expected to be different. An estimate based on a McConnell–Strathdee type analysis yields: $\mathrm{Tr}(A'_D{}^2) = 0.04 - 0.4$ MHz^2, $\mathrm{Tr}(A'_H{}^2) = 24$ MHz^2 (β – H), $\mathrm{Tr}(A'_C{}^2) = 370$ MHz^2 (β-^{13}C) and 3300 MHz^2 (α,γ-^{13}C). These values are responsible for the different nuclear relaxation rates W_N, for the cross-relaxation rates W_x in **2c** and **2d**, and also for the saturation behavior of the nuclear and—in part—of the electron spin transitions. In the following the experimental requirements will be discussed for the labeled radicals **2c** and **2d** and the different nuclei present in these compounds.

Saturation Behavior of Electron Spin Transitions. The ESR saturation parameter $\sigma_e = (1/4)\gamma_e^2B_e^2\Omega_eT_{2e}$ includes the magnetogyric ratio of the electron γ_e, the effective microwave (mw) field at the sample B_e, Freed's saturation parameter for the electron transitions Ω_e, and the reciprocal homogeneous ESR line width T_{2e}.[38] The required saturating mw field for $\sigma_e \cong 1$ is determined by the magnitude of the product Ω_eT_{2e}. If the g-factor anisotropy and the spin-rotational interaction are small, the dependence of these parameters on the anisotropic hyperfine interactions of the different nuclei present in the radical is no longer negligible. Introduction of nuclei like ^{13}C in positions of high spin density might therefore result in larger electron spin-lattice relaxation rates, $W_e \approx 2/\Omega_e$, and also in larger line widths.

Actually, in the system under study larger ESR line widths are observed for **2d** as compared to those of **2c** and increased mw fields B_e are required to saturate the electron spin transi-

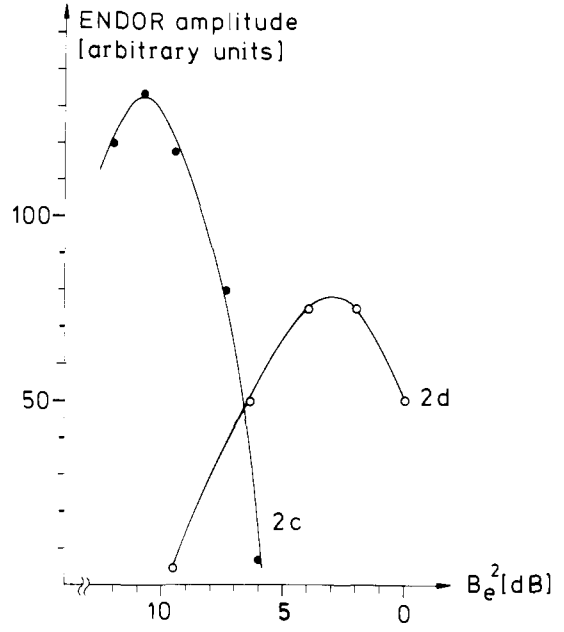

Figure 6. ENDOR amplitudes of the high-frequency proton lines in radicals **2c** and **2d** as a function of the microwave power (dB of attenuation, 200-mW klystron) at the same experimental conditions (see Figure 4, caption). The relative magnitudes of amplitudes are not correlated; the signal-to-noise ratio has been considerably better for **2c.**

tions of the former in order to obtain a sufficient ENDOR effect. Figure 6 shows the ENDOR amplitudes of the high-frequency proton lines of **2c** and **2d** as a function of the mw power (dB of attenuation, 200-mW klystron).[39] It is demonstrated that maximum ENDOR amplitudes are obtained using 11 dB (16 mW) for radical **2c** and 3 dB (100 mW) for radical **2d.** The value of **2c** equals that used for radical **2a** within experimental error. It has to be noted that these mw power data are derived from the attenuated power output of the klystron; hence, they do not represent directly the effective mw field at the sample place. An estimate recently published for a comparable experimental arrangement showed that for 200-mW power the effective field B_e amounts only to 0.01 mT (rotating frame).[40]

Saturation Behavior of Nuclear Spin Transitions. Similar to the saturation of electron spin transitions, the saturation condition for the nuclear spin transitions $\sigma_N = (1/4) \cdot \gamma_N^2 B_N^2 \Omega_N T_{2N} \geq 1$ is important for ENDOR spectroscopy; γ_N is the magnetogyric ratio of the respective nucleus, T_{2N} the ENDOR line width parameter, Ω_N Freed's nuclear spin-lattice relaxation parameter,[38] and B_N the effective radio frequency (rf) field at the nucleus ($B_N = \kappa B_N'$, where B_N' is the external rf field, and $\kappa = \nu_{ENDOR}/\nu_N$, the hyperfine enhancement factor[23]). Comparing different nuclei in the same radical, the nuclear spin relaxation rates $W_N \approx 2/\Omega_N$ are essentially determined by the electron-nuclear dipolar interaction, i.e., $\mathrm{Tr}(A'^2)$. Consequently, besides the magnetogyric ratio and the hyperfine enhancement factor $\mathrm{Tr}(A'^2)$ constitutes the main factor in the determination of the rf fields required for an optimum ENDOR effect.

A closer inspection for protons and deuterons shows that one should be able to saturate both equally well since $T_{2H} \approx T_{2D}$ and Ω_N is increased proportional to $(\gamma_H/\gamma_D)^2$.[8] This does not hold for the ^{13}C nucleus because $(\gamma_H/\gamma_C)^2 = 15.8$ and, additionally, $\mathrm{Tr}(A'^2_C)$ is often much larger than $\mathrm{Tr}(A'^2_H)$. In the present case, this latter effect amounts to about one (**2c**) or two (**2d**) orders of magnitude (vide supra). Fortunately, the hyperfine enhancement factor of carbon-13 is very large (high-frequency ENDOR lines: **2c,** 5.8; **2d,** 6.6); thus saturation of the NMR transitions can be achieved.

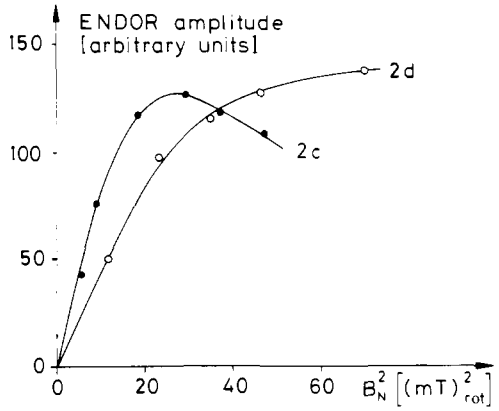

Figure 7. ENDOR amplitudes of the high-frequency ^{13}C ENDOR lines in radicals **2c** and **2d** as a function of the squared effective NMR field B_N^2 at the nucleus. The amplitudes of **2c** and **2d** are not comparable, since experimental conditions had to be changed for the detection of the ^{13}C ENDOR lines in **2d,** toluene (330 K, rf modulation (10 kHz) amplitude = 100 kHz, microwave power 100 mW).

We have measured the effective ENDOR amplitudes of the high-frequency ^1H, ^2H, and ^{13}C resonance lines of the radicals **2c** and **2d** as function of the rf power. For the proton and the deuterons in both radicals the plots proved to be identical within experimental error; a maximum ENDOR effect occurs at $B_N = (1.5 \pm 0.1)$ mT (rotating frame). In Figure 7 the saturation behavior of the ^{13}C ENDOR amplitudes of **2c** and **2d** is compared.[39] As expected for carbon-13 in positions of high spin density (α,γ; **2d**), saturation can hardly be achieved with effective fields up to $B_N = 8.5$ mT ($B_N' = 1.3$ mT, rotating frame), whereas the ^{13}C line of the β position (**2c**) is already saturated at about $B_N = 5.0$ mT ($B_N' = 0.87$ mT, rotating frame).

Temperature Dependence of ENDOR Amplitudes. For different kinds of nuclei with different nuclear relaxation rates W_N—due to different electron-nuclear dipolar contributions $\mathrm{Tr}(A'^2)$—optimum ENDOR signals are expected at different temperatures. We have measured the ENDOR enhancement of radical **2c** observing the high-frequency ^1H, ^2H, and ^{13}C ENDOR lines from 300 up to 380 K (mineral oil). In this range the ESR signal increases almost linearly by about a factor of 4, obviously caused by the increased homolysis of the dimer of **2c.** This effect has, of course, been taken account of in the study of the ENDOR enhancements, yielding maximum values for ^2H at (330 ± 3) K, for ^1H at 340 K, and for $^{13}C_\beta$ at 360 K; see Figure 8. The temperatures necessary for an optimum ENDOR effect are somewhat higher than those usually required[41] because of the large radius r of the radicals studied influencing the rotational correlation time $\tau_c = 4\pi r^3\eta/3kT$. The results for the different nuclei (Figure 8) reflect the increasing electron-nuclear dipolar interaction from ^2H to ^1H and ^{13}C. It is to be noted that the magnitudes of the ENDOR amplitudes in Figure 8 are not directly comparable, since the experimental conditions have been kept constant over the whole frequency range rather than having been optimized for each individual line. As a result almost equal signal intensities of all three resonances were obtained at about 360 K; see the multinuclear ENDOR spectrum pictured in Figure 4.

A detection of the ENDOR signals due to ^{13}C in the α,γ positions of radical **2d** was only possible at temperatures above 400 K in the mineral oil used, whereas the optimum temperatures for the protons and deuterons are not considerably changed as compared to **2c.** In toluene solution, the optimum temperature for ^{13}C ENDOR was found to be about (315 ± 5) K. However, the influence of the electron-nuclear dipolar interaction and the temperature-dependent dimerization process on W_e presents a very complex situation which does

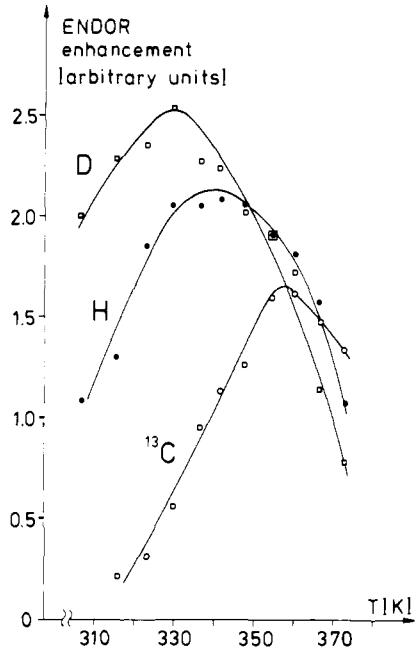

Figure 8. ENDOR enhancements for the respective high-frequency ENDOR lines of ^{1}H, ^{2}H, and ^{13}C in the radical **2c** as function of temperature. For experimental conditions, refer to Figure 4, caption.

not allow a quantitative comparison of the relaxation behavior of radicals **2c** and **2d.**

Electron–Nuclear Cross-Relaxation Effects. Cross-relaxation processes W_{x1} (flip flop) and W_{x2} (flop flop) of electron and nuclear spins are also caused by modulation of the electron–nuclear dipolar interaction. Since $W_{x1,2} \propto \mathrm{Tr}(A'^2)/\tau_c$ holds in the slow tumbling limit ($\omega_x^2\tau_c^2 \gg 1$, $\omega_e \approx \omega_x$), increasing contributions from cross relaxations ($W_{x1,2} > W_N$) are expected at higher temperatures. An additional W_{x1} process might be derived from the modulation of the isotropic hyperfine couplings in the radical by internal rotation or by the dimerization process with different correlation times. The detection of such processes and a discrimination between them can be achieved by studying ENDOR amplitudes as a function of individual m_I components in the ESR spectrum selectively saturated at different temperatures; see, e.g., ref 12 and 42.

In radical **2c** no cross-relaxation effects of ^{13}C could be observed in mineral oil up to 380 K, whereas they were detectable in toluene above room temperature (amplitude ratio about 2 at 325 K). Considering the small ^{13}C anisotropy in the β position, it is not surprising that these effects are not very pronounced, compare, e.g., ref 11. For radical **2d** a dominant W_{x2} process was clearly established arising from the modulation of the large anisotropic ^{13}C hyperfine coupling in the α,γ positions. The magnitude of this effect is comparable to that observed for the triphenylmethyl radical, labeled at the central carbon.[12]

Conclusions

As has been demonstrated, the extensions of ENDOR from protons to nonprotons and from isotropic solutions to liquid crystals provide valuable additional information. In particular, the smectic phase ENDOR studies allow accurate measurements of the hyperfine coupling constant shifts. Including the ^{13}C ENDOR studies, some conclusions concerning the twist angles of the bis(biphenylenyl)propenyl radicals could be drawn. Thereafter, the twist angles proposed in a recent paper have to be revised. Our studies on the deuterated compounds revealed two interesting aspects, i.e., a significant isotope effect affecting the largest (β proton) splitting when replacing ^{1}H by ^{2}H in the biphenylenyl moieties and a quadrupole splitting of the deuterons observable in the liquid crystals by means of ENDOR.

The presence of different kinds of magnetic nuclei in one molecule enabled us to study their different relaxation behavior and the consequences with regard to the ENDOR response. Probably the most striking result is the possibility of simultaneously recording several different magnetic nuclei in one molecule over a wide NMR frequency range. Since bis(biphenylenyl)propenyl exhibits high stability in the solid state (dimer) and in solution, we propose the respectively labeled form of this radical as a *multinuclear ENDOR standard*, advantageously to be used in a liquid crystal as solvent. This standard provides particular merits for probing the engineering efficiency of a liquid-phase ENDOR arrangement over the range of 1 to 35 MHz including frequency stability, power of the rf source, and resolution.

Acknowledgments. H. K. wishes to thank the Deutsche Forschungsgemeinschaft and the Fonds der Chemischen Industrie for financial support. We especially want to acknowledge Professor K. H. Hausser's active support of the collaboration between the Free University of Berlin and the Max-Planck-Institut of Heidelberg.

References and Notes

(1) Max-Planck-Institut für Medizinische Forschung, Abteilung für Molekulare Physik, 6900 Heidelberg, West Germany.
(2) Koelsch, C. F. *J. Am. Chem. Soc.* **1957**, *79*, 4439.
(3) Watanabe, K.; Yamauchi, J.; Ohya-Nishiguchi, H.; Deguchi, Y. *Bull. Chem. Soc. Jpn.* **1974**, *47*, 274.
(4) Hausser, K. H. *Z. Naturforsch. A* **1962**, *17*, 158.
(5) Berndt, A. *Tetrahedron* **1969**, *25*, 37.
(6) Watanabe, K. *Bull. Chem. Soc. Jpn.* **1975**, *48*, 1732.
(7) Möbius, K.; Biehl, R. In "Multiple Electron Resonance Spectroscopy"; Dorio, M. M., Freed, J. H., Eds.; Plenum Press: New York, 1979.
(8) Biehl, R.; Lubitz, W.; Möbius, K.; Plato, M. *J. Chem. Phys.* **1977**, *66*, 2074.
(9) Kirste, B.; Kurreck, H.; Fey, H.-J.; Hass, Ch.; Schlömp, G. *J. Am. Chem. Soc.*, in press.
(10) Kirste, B. *Chem. Phys. Lett.* **1979**, *64*, 63.
(11) Kirste, B.; Kurreck, H.; Lubitz, W.; Schubert, K. *J. Am. Chem. Soc.* **1978**, *100*, 2292.
(12) Fey, H.-J.; Lubitz, W.; Zimmerman, H.; Plato, M.; Möbius, K.; Biehl, R. *Z. Naturforsch. A* **1978**, *33*, 514.
(13) Kuhn, R.; Fischer, H.; Neugebauer, F. A.; Fischer, H. *Justus Liebigs Ann. Chem.* **1962**, *654*, 64.
(14) Burr, J. G., Jr. *J. Am. Chem. Soc.* **1951**, *73*, 823.
(15) Kuhn, R.; Neugebauer, F. A. *Monatsh. Chem.* **1964**, *95*, 3.
(16) Pavlyuchenko, A. I.; Smirnova, N. I.; Kovsher, E. I.; Titov, V. V.; Purvanetskas, G. V. *Zh. Org. Khim.* **1976**, *12*, 1054.
(17) Fey, H.-J.; Kurreck, H.; Lubitz, W. *Tetrahedron* **1979**, *35*, 905.
(18) Dalal, N. S.; Kennedy, D. E.; McDowell, C. A. *J. Chem. Phys.* **1974**, *61*, 1689.
(19) Biehl, R.; Hass, Ch.; Kurreck, H.; Lubitz, W.; Oestreich, S. *Tetrahedron* **1978**, *34*, 419.
(20) Hinrichs, K.; Kirste, B.; Kurreck, H.; Reusch, J. *Tetrahedron* **1977**, *33*, 151.
(21) Kirste, B.; Kurreck, H.; Harrer, W.; Reusch, J. *J. Am. Chem. Soc.* **1979**, *101*, 1775.
(22) Kevan, L.; Kispert, L. D. "Electron Spin Double Resonance Spectroscopy"; Wiley: New York, 1976.
(23) Geschwind, S. In "Hyperfine Interactions"; Freeman, A. J., Frankel, R. B., Eds.; Academic Press: New York, 1967.
(24) Karplus, M.; Fraenkel, G. K. *J. Chem. Phys.* **1961**, *35*, 1312.
(25) Whiffen, D. H. *Mol. Phys.* **1963**, *6*, 223.
(26) Luckhurst, G. R. *Mol. Phys.* **1966**, *11*, 205.
(27) Horsfield, A.; Morton, J. R.; Whiffen, D. H. *Mol. Phys.* **1961**, *4*, 425.
(28) Stone, E. W.; Maki, A. H. *J. Chem. Phys.* **1962**, *37*, 1326.
(29) Krusic, P. J.; Meakin, P.; Jesson, J. P. *J. Phys. Chem.* **1971**, *75*, 3438.
(30) Reddoch, A. H.; Dodson, C. L.; Paskovich, D. H. *J. Chem. Phys.* **1970**, *52*, 2318.
(31) Das, T. P. *J. Chem. Phys.* **1957**, *27*, 763.
(32) Falle, H. R.; Luckhurst, G. R. *J. Magn. Reson.* **1970**, *3*, 161.
(33) Luckhurst, G. R. In "Liquid Crystals and Plastic Crystals"; Gray, G. W., Winsor, P. A., Eds.; Ellis Horwood: Chichester, 1974; Vol. 2, p 144.
(34) Luckhurst, G. R.; Poupko, R. *Mol. Phys.* **1975**, *29*, 1293.
(35) McConnell, H. M.; Strathdee, J. *Mol. Phys.* **1959**, *2*, 129.
(36) Atherton, N. M. "Electron Spin Resonance"; Ellis Horwood: Chichester, 1973.
(37) Falle, H. R.; Whitehead, M. A. *Can. J. Chem.* **1972**, *50*, 139.
(38) Freed, J. H. In "Electron Spin Relaxation in Liquids"; Muus, L. T., Atkins, P. W., Eds.; Plenum Press: New York, 1972; p 503.

(39) For a theoretical description of the dependences of ENDOR amplitudes on the mw or rf power, see: van der Drift, E.; Danners, A. J.; Smidt, J.; Plato, M.; Möbius, K., submitted for publication.
(40) Lendzian, F. Diplomarbeit, FU, Berlin, 1978.
(41) Biehl, R.; Hass, Ch.; Kurreck, H.; Lubitz, W.; Oestreich, S. *Tetrahedron* **1978**, *34*, 419.
(42) Lubitz, W.; Dinse, K. P.; Möbius, K.; Biehl, R. *Chem. Phys.* **1975**, *8*, 371.

Electron Nuclear Double Resonance Spectra of Stellacyanin, a Blue Copper Protein

James E. Roberts,[1a] Theodore G. Brown,[1a] Brian M. Hoffman,*[1a] and Jack Peisach[1b]

Contribution from the Department of Chemistry, Northwestern University, Evanston, Illinois 60201, and the Department of Pharmacology, Albert Einstein College of Medicine of Yeshiva University, New York, New York 10461. *Received June 18, 1979*

Abstract: The ^{1}H, ^{14}N, and $^{63,65}Cu$ electron nuclear double resonances (ENDOR) of stellacyanin have been measured. This represents the first published observation of copper ENDOR in a protein. In confirmation of the results of Rist et al.,[13] the cupric ion must have a minimum of two nitrogenous ligands. The Cu hyperfine splitting (hfs) tensor and the quadrupole tensor have been determined, the first such complete characterization for a copper protein. The unusual Cu hyperfine tensor can be explained by assuming a flattened tetrahedral geometry, without assumption as to the nature of the coordinated ligands; the observation of large quadrupole couplings also appears to be an effect of geometry. The coordination of Cu in stellacyanin is discussed in terms of these results.

Introduction

The blue copper proteins contain a mononuclear Cu(II) site that has unusual optical and magnetic properties.[2a] The electronic spectrum is characterized by a very intense absorption near 600 nm with a molar extinction coefficient of the order 10^3-10^4, in contrast to the low molar extinctions of ordinary mononuclear copper complexes, ~1-100. Typically, the EPR spectrum is also quite different from that observed for "normal" copper; the g tensor is nonaxial and both A_z^{Cu}, the copper hyperfine splitting (hfs) constant associated with the largest g value, and A_{iso}^{Cu}, the isotropic coupling, show unusually small values.

On the basis of near-infrared and visible absorption and circular dichroism spectroscopy[2b] and pulsed EPR data,[3] a distorted tetrahedral coordination geometry has been proposed for the blue copper site. It has further been suggested, partially from model compound studies,[4,5] that the intense blue color is due to S → Cu charge-transfer transitions[2b,6] and that the unpaired electron is substantially delocalized onto a sulfur ligand, accounting for the low values of A_z^{Cu}.[7]

For two blue copper proteins, plastocyanin[8] and azurin,[9] the proposal regarding structure has been substantiated by single-crystal X-ray diffraction. In both, the copper is coordinated by nitrogens from two histidines and sulfur atoms, one from methionine and the other from cysteine. The CuN_2S_2 chromophore exhibits distorted tetrahedral stereochemistry. It is perhaps tempting to generalize this arrangement to include other blue copper centers. However, not all of the blue proteins contain methionine; stellacyanin is the typical example in which it is absent.[10]

Stellacyanin[10] is a blue copper protein of no known function. It is obtained from the bark of *Rhus vernicifera*, the Japanese Lac tree, has a molecular weight of ~20 000, and contains one copper atom per molecule. The detailed electronic spectra and EPR have been reported.[10,11] Only one of the copper hyperfine couplings can be determined unambiguously from the EPR, and then only at the Q-band (35 GHz).[11] The other two principal values of the hfs tensor have been determined by linewidth analyses, and conflicting values were obtained.[10,11] Pulsed EPR studies have confirmed that histidine is bound to copper;[12] the presence of two nitrogen ligands was indicated by ENDOR experiments,[12] although the discussion in the published report is somewhat sketchy. This study was also limited in frequency range because of the instrument used, and thus copper ENDOR was unobservable.

In order to more completely define the coordination sphere in stellacyanin, we have reinvestigated its ENDOR. The results of Rist et al.[13] are confirmed, and show that copper has at least two nitrogen ligands; if there is a third nitrogenous base, then two of these ligands must be related by an approximate inversion center. The complete copper hyperfine splitting (hfs) tensor has been determined, resolving the discrepancy between the published values; in addition, the quadrupole splitting tensor has been obtained. These measurements, along with others under way in our laboratory, constitute the first observation of ENDOR from copper, and have allowed the first such complete characterization of the magnetic properties of a blue copper center.

Experimental Section

A sample of stellacyanin in 0.01 M potassium phosphate buffer (pH 7.0), with a copper concentration of ~3 mM, was prepared as discussed elsewhere.[10] ENDOR was observed more readily when this sample was diluted 50% with glycerol. ENDOR experiments were performed at temperatures near 5 K using a Helitran LTD3-110 variable temperature system, and below the λ point of liquid helium by immersing the microwave cavity in a bath of superfluid helium. Both Dewar systems and the ENDOR spectrometer employing 100-kHz detection are described elsewhere.[14] Copper ENDOR was observed using a Waveter Model 2001 signal generator as the radiofrequency source. ^{14}N and Cu ENDOR spectra were obtained by monitoring the dispersion component of the EPR signal at 2.0 K, and ^{1}H and Cu ENDOR were observed at both 2 and 5 K while monitoring the absorption EPR signal. The EPR saturation behavior was essentially Lorentzian,[15] although considerable mixing of dispersion and passage components into the absorption signal was observed at most microwave powers (>~ 0.2 μW). ENDOR spectra were obtained under the following conditions: 2-μW (2 K) and 0.2-mW (5 K) microwave power, a 100-kHz field modulation amplitude of 3-4 G, and radiofrequency (rf) field strength of ~1 G in the rotating frame.

0002-7863/80/1502-0825$01.00/0